Applied Geochemistry 193 (2025) 106579

Contents lists available at ScienceDirect

Applied Geochemistry

journal homepage: www.elsevier.com/locate/apgeochem

Sorption of Eu(III) on C–S–H phases in the presence of gluconate: A molecular dynamics study

Iuliia Androniuk *, Rosa Ester Guidone, Marcus Altmaier, Xavier Gaona

Institute for Nuclear Waste Disposal (INE), Karlsruhe Institute of Technology (KIT), Karlsruhe, Germany

ARTICLE INFO

Keywords:
C–S–H
Europium
Gluconate
Surface sorption
Molecular dynamics

ABSTRACT

Cement is a key barrier material in radioactive waste repositories, where calcium-silicate-hydrate (C–S–H) phases play a central role in immobilizing cationic radionuclides. However, organic ligands, originating from additives or waste, can enhance radionuclide mobility by forming soluble complexes and competing for surface sorption. In this study, a surface model was developed that combines experimental observations with theoretical insights into C–S–H structure, enabling detailed sampling of the most probable sorption sites. Molecular dynamics (MD) simulations and potential of mean force (PMF) calculations were used to develop molecular-scale understanding of how organic additives influence the adsorption and mobility of trivalent actinides and lanthanides in cementitious materials. Eu(III) was considered as a model of key trivalent radionuclides expected in nuclear waste, *i.e.* Pu(III) and Am(III), based on their similar charge-to-size (z/d) ratios, and gluconate was chosen as a model organic ligand. The results from the Eu(III)/C–S–H binary system confirmed strong sorption and showed that the most common sorption sites are the deprotonated silanol groups of the surface. Results obtained for the binary system are in line with Time Resolved Laser Fluorescence Spectroscopy data available for Eu(III) and Cm (III). Depending on gluconate concentration, two main effects on Eu(III) uptake on the C–S–H phases have been found: (a) sorption of the 1:1 Eu(III)-GLU complex at low ligand concentration; (b) formation of a stable ternary Ca–Eu(III)-GLU aqueous complex that does not sorb at high ligand concentration. It is important to consider formation of the ternary complex C–S–H/Eu(III)/GLU for the overall interpretation and understanding of the system.

1. Introduction

Cement is the most important and extensively used construction material. Due to its structural functionalities and high retention capabilities, cement is considered to be an important component within the multibarrier system in the design and construction of repositories for radioactive waste. It serves various roles, such as being the main construction material, a part of the packaging for certain waste types, and a sealing material for storage cells (Glasser et al., 1989). Calcium silicate hydrate (C–S–H) is a major hydration product, constituting 50–70 % of the mass, and the main binding phase of Portland cement that contributes to its strength and durability. It is a nanocrystalline material with a wide range of chemical compositions and high surface area. The C–S–H phases are considered as the main sink of metal ions in cement, and thus were chosen as a model in this study (Evans, 2008; Wieland, 2014; Ochs et al., 2016). Accurate molecular-level modeling of C–S–H phases is challenging, typically requiring large simulation cells and extended simulation times to achieve the desired statistical accuracy (Duque-Redondo et al., 2022). Molecular modelling is usually done with defect tobermorite as the closest mineral structure (Kirkpatrick et al., 1997; Grangeon et al., 2017).

Organic molecules can be introduced into a waste repository both as part of the cement material and as constituents of the waste itself. The presence of organic ligands introduces a potential concern, as these molecules may enhance the mobility of radionuclides by increasing their solubility and/or decreasing their uptake by mineral phases (Keith-Roach, 2008; Fralova et al., 2021). Therefore, it is crucial to understand the sorption and complexation behavior of organic molecules in cementitious systems. In cement production, gluconate (GLU) is commonly used as a dispersing and retarding additive, and it could also be present in the radioactive waste after being used as complexing agent (Keith Roach and Shahkarami, 2021). Gluconate was chosen as a model

This article is part of a special issue entitled: Migration 2023 published in Applied Geochemistry.

* Corresponding author.
E-mail address: iuliia.androniuk@kit.edu (I. Androniuk).

https://doi.org/10.1016/j.apgeochem.2025.106579
Received 11 March 2024; Received in revised form 9 September 2025; Accepted 26 September 2025
Available online 27 September 2025

molecule in this study. It is a hydroxycarboxylate that is stable in high alkaline media, forms strong chelate complexes with metal ions, and sorbs well on cement surfaces.

In this study, Eu(III) has been selected as a model radionuclide. It is representative of key trivalent actinides and lanthanides expected in nuclear waste, namely Pu(III) and Am(III), based on their similar charge-to-size (z/d) ratios, coordination chemistry and complexation behavior. The sorption of Eu(III) on cementitious materials has already been assessed in a number of experimental studies. These investigations have revealed rapid sorption kinetics (steady state was reached within 1 day) and strong uptake (with reported high distribution ratios, $R_d \approx 10^6$ dm^3/kg) driven by two primary mechanisms: surface sorption on silanol groups and incorporation into the interlayer and the CaO layer of C–S–H (Pointeau et al., 2001; Tits et al., 2003; Schlegel et al., 2004; Dario et al., 2006).

Recent study has established that gluconate has no discernible impact on the sorption of Eu(III) on C–S–H with low Ca/Si ratio (Dettmann et al., 2023). However, under high-pH conditions and elevated Ca^{2+} concentrations, a reduction in the uptake of trivalent radionuclides has been observed in the presence of gluconate (Wieland, 2014; Guidone, 2023, 2024). Despite these observations, the precise molecular mechanism underlying this phenomenon remains insufficiently defined.

Molecular dynamic simulations serve as a powerful tool for investigating the atomic-scale behavior and properties of cement interfaces, providing valuable insights that complement and explain experimental observations. This approach has gained widespread acceptance and proven its utility as an effective method for examining complex sorption processes in cementitious environments (e.g. Androniuk and Kalinichev, 2020; Duque-Redondo et al., 2021; Tu et al., 2021; Masara et al., 2023). In this study, classical molecular dynamics (MD) simulations and the potential of mean force (PMF) calculations were used to gain a mechanistic understanding of surface sorption processes. The primary objective of this modelling study is to understand molecular interactions in the ternary system C–S–H/Eu(III)/gluconate, aiming to enhance interpretation of the experimental data.

2. Computational methods

The C–S–H surface was modeled based on the crystal structure of defected tobermorite, which has been established as the closest structure to real cement hydrate (Kirkpatrick et al., 1997; Grangeon et al., 2016, 2017; Kumar et al., 2017; Kunhi Mohamed et al., 2018). The atomistic model of the surface was built from the initial structure of tobermorite 14 Å ($Ca_5Si_6O_{16}(OH)_2{\cdot}7H_2O$) (Bonaccorsi et al., 2005). The layered structure of tobermorite is composed of sheets of sevenfold coordinated calcium cations with silicate chains on both sides. The interlayer space contains additional calcium cations and water molecules. The crystallographic unit cell has been multiplied ($8 \times 8 \times 2$) to create a relatively large simulation supercell to accumulate better statistical data. The simulation cell was then cleaved in the middle of interlayer along the (0 0 1) crystallographic plane to form a basic model of the C–S–H surface. As a next step, defects and adjustments were made to the cleaved surface to create a C–S–H model typical for a Ca/Si ratio of 1.4, with initial dimensions of $54 \times 54 \times 100$ Å^3 (a triclinic cell with $\alpha = \beta = 90°$, and $\gamma = 66.5°$, including a vacuum gap).

The real C–S–H phases are highly heterogeneous, with variable Ca/Si ratios, disorder in the silicate chains, and a broad distribution of interlayer environments. These features are only present partially in the model. As a result, the sorption sites, hydration states, and dynamic behavior observed in simulations may not fully represent the diversity of environments present in real cement systems (Duque-Redondo et al., 2022). Therefore, results of our modeling should be regarded as qualitative trends rather than universally transferable predictions for all C–S–H compositions and structures.

Experimental studies on C–S–H phases with a high Ca/Si ratio (>1.4) show that the mean chain length in the silicate layer is expected to be around 2.3. Subsequently, the bridging Si tetrahedra were randomly deleted in accordance with available experimental NMR and IR data (Cong and Kirkpatrick, 1996; Beaudoin et al., 2009; Roosz et al., 2018), and additional Ca^{2+} and OH^- ions were introduced. The silanol groups of the bridging Si and one of the pairing Si were deprotonated based on the expected protonation state of the surface at high pH (Churakov et al., 2014). The deprotonated oxygens of the surface were assigned a partial charge of $q_{onb} = 1.3|e|$, higher than the protonated ones in the standard ClayFF force field, similar to the charge used for the NBO (non-bridging oxygens) of the silicate groups in the alkali silicate hydrate gel (Kirkpatrick et al., 2005a, 2005b). The extended gap between the cleaved surfaces was filled with solution molecules. The final simulation box included: 816 Si atoms, 767 structural Ca atoms, 377 Ca^{2+} ions, 2016 bridging O atoms, 672 non-bridging O atoms, 48 surface hydroxyl O and H atoms, 149 aqueous O atoms, 7613 water O atoms, 15375 H atoms.

The interaction parameters for the surface were taken from the ClayFF force field, known for their reliability and accuracy in cement/water interface simulations (Cygan et al., 2004, 2021; Kalinichev et al., 2007). For the gluconate molecule, parameters were sourced from the OPLS force field, which is compatible with ClayFF (Jorgensen et al., 1996; Szczerba and Kalinichev, 2016; Zhao et al., 2024), and partial charges were calculated through CHelpG fitting of the electrostatic potentials from the HF/6-31G* calculations in Gaussian software package (version g16.C.01, Frisch et al., 2016). Water was modeled using the extended simple point charge (SPC/E) model (Berendsen et al., 1987). Parameters for Eu(III), that have been proved to be compatible with the organic force fields, were taken from Veggel and Reinhoudt, 1999).

Standard Lorenz−Berthelot mixing rules were applied to calculate short-range Lennard-Jones interactions between unlike atoms, using a cut-off distance of 14 Å. Long-range electrostatic forces were evaluated using the Ewald summation method. All molecular dynamics simulations were performed using the LAMMPS software package (September 29, 2021 version; Plimpton, 1995). The equilibration of the model system was carefully monitored by evaluating the system's temperature, pressure, kinetic, and potential energy, and dimensions of the simulation box, to verify that these parameters reach their equilibrium steady-state values on average, ensuring that the system accurately represented the desired conditions (Braun et al., 2019). These steady-state values were already observed after ~300 ps, but it was decided to use 5 ns intervals to further ensure accuracy.

The C–S–H surface was equilibrated for 5 ns in the NPT ensemble prior to introducing Eu(III) and gluconate into the interface solution. The Newtonian equations of the atomic motions were then numerically integrated with a timestep of 1 fs. The model systems were initially equilibrated for 5 ns in the isobaric−isothermal statistical ensemble (NPT) and subsequently for 5 ns in the canonical ensemble (NVT). Temperature and pressure were constrained using the Nose−Hoover thermostat and barostat under ambient conditions (T = 295 K, P = 0.1 MPa).

To prevent drifting of the modeled systems, four Si atoms from each silicate layer were immobilized during NVT production runs, though they were still allowed to interact with other atoms. The VMD software package (version 1.9.3) has been used for visualization of the simulation trajectories (Humphrey et al., 1996).

The potential of mean force (PMF) calculations is a computational technique used in molecular dynamics simulations to estimate the free energy as a function of a reaction coordinate or a specific set of collective variables. It provides insights into the energy landscape of a system, helping to understand the thermodynamics of a process or the stability of different states. In this study, PMF calculations were applied to quantitatively describe the adsorption free energy profiles of Eu(III) and Eu(III)/GLU complexes as a function of their distance from the C–S–H surface.

The "umbrella sampling" algorithm was used to sample rarely visited atomic configurations of the system with statistical accuracy that would

be unattainable through standard MD simulations (Kastner, 2011). In this technique, biasing potentials are applied to enhance sampling in specific regions. While highly precise, this method is computationally expensive. Therefore, only the most typical sorption sites on the (001) surface of C–S–H were selected (Androniuk and Kalinichev, 2020; Chiorescu et al., 2022): the bridging site (deprotonated silanol group of the bridging Si), the defect site (deprotonated silanol groups of pairing Si), the silicate chain site, and the interchain site (the space between the silicate chains on the surface) (see Fig. 1).

A complete PMF calculation involves multiple independent molecular dynamics simulations with biasing potentials applied along the chosen reaction coordinate. For each obtained PMF curve, approximately 100 biased MD simulations were run in the *NVT* ensemble, each lasting 2 ns, to cover the complete reaction coordinate. The *z*-distance between the topmost oxygens of the surface and europium was selected as the collective variable. Additional weak *xy* constraints were applied as a "soft cylindrical wall" of a small diameter to maintain Eu(III) position on top of the sorption site.

The umbrella sampling calculations were performed using the COLVARS module integrated into the LAMMPS software package (Fiorin et al., 2013). The weighted histogram analysis method (WHAM) was employed to compute the free energy profiles along the reaction coordinate from the umbrella sampling data. All simulations for each constrained distance window are independent and were run in parallel. The Monte Carlo bootstrapping approach implemented in the WHAM algorithm was used to calculate statistical uncertainties (Grossfield, 2014; Grossfield et al., 2018).

3. Results and discussion

3.1. Eu(III) sorption on C–S–H

The uptake of Eu(III) on C–S–H phases and cement has been investigated through multiple sorption and spectroscopic studies. It has been confirmed that C–S–H is the main responsible phase for europium's retention, with sorption on the surface and incorporation identified as the two major uptake mechanisms (Pointeau et al., 2001; Tits et al., 2003; Schlegel et al., 2004). In this study, the incorporated species are not considered due to their strong immobilization in the structure, rendering them inaccessible to the solution and, consequently, unavailable for interaction with organics on the solid-solution interface.

Understanding the sorption mechanism of Eu(III) in binary systems serves to validate the chosen theoretical method and provides a reference for interpreting results in more complex systems where organic molecules are present. In high pH solutions, typical for cement systems (pH ~ 13, Guidone et al., 2024), $Eu(OH)_3(aq)$ is considered to be the dominating aqueous species (Pointeau et al., 2001; Giffaut et al., 2014). Therefore, it was selected for this MD study.

Fig. 2 shows the results of the potential of mean force calculations for Eu(III) sorption on the defect, bridging, and chain sorption sites. Sorption on the interchain site, that is a probable site for cations on the C–S–H surfaces (such UO_2^{2}; Chiorescu et al., 2022) have been also evaluated, nevertheless, Eu(III) was strongly attracted to the defect site (which would be a part of the interchain site, given the high number of defects on the surface). This suggests that the interchain site may not be a typical sorption site for Eu(III) in these conditions, because of the high energy needed to replace multiple hydroxyl groups in europium's coordination sphere with surface hydroxyls. For the other three sites, a stable sorption surface configuration can be identified. Low minima for the defect and bridging sites are observed very close to the surface at distances 1.9 Å and 2.1 Å, respectively. The energy barriers for desorption are also relatively high with an energy difference of around 60 kJ/mol, further indicating a more favorable sorption for these two sites. This finding supports the notion that Eu(III) forms strong inner-sphere complexes on the C–S–H surface, as previously reported in the literature (Pointeau et al., 2001; Schlegel et al., 2004). The strength of Eu(III) binding, calculated with PMF, is similar to those of Ca^{2+} at the same sorption site (Androniuk and Kalinichev, 2020) and validates the experimental findings. Meanwhile, the closest minimum for the chain site is at a distance of around 4 Å with a much lower energy barrier of approximately $\Delta G = 25$ kJ/mol, corresponding to sorption as a weaker outer-sphere complex.

The running coordination numbers for Eu(III) pairs were calculated from the trajectories at the positions of the lowest energy minima, as presented in Fig. 3. The results indicate that Eu(III) was sorbed on the defect site through coordination with two deprotonated silanol groups and on the bridging site through coordination with one deprotonated silanol group. The total coordination number of the adsorbed Eu(III) is approximately 7, which is lower than in the pure aqueous solution (typically CN = 8–9; Marmodee et al., 2010) due to hindrances caused by the surface and the presence of negatively charged aqueous hydroxyl groups in the first coordination sphere.

It can be seen that surface complexes are formed through the replacement of water molecules and hydroxyls in the first coordination sphere by oxygens of the deprotonated silanol groups. Initially, there are around 4 water molecules and hydroxyls each, as seen in the outer-sphere complex (Fig. 3 – CH-4.2 Å). Approximately 1.3 water molecules and 4 hydroxyls remain in the inner-sphere complex formed on the bridging site (Fig. 3 – BR-2.3 Å), and these numbers are further reduced to 2 water molecules and 3 hydroxyls for the defect site complexation (Fig. 3 – DEF-1.8 Å). The results of spectroscopic studies by Pointeau et al. (2001) and Tits et al. (2003) have shown that the sorbed Eu(III)/Cm(III) species have a reduced hydration sphere. Further analysis of lifetimes of the surface species during TRLFS experiments allowed to identify the presence of approximately 1.4 water molecules in the first hydration sphere of Cm(III) and Eu(III), which is in good agreement with the results of our MD study.

Ca^{2+} cations are identified in the second coordination sphere of Eu(III) at $d_{Eu\text{-}Ca}$ = 3.2–3.5 Å, and they play a crucial role in the sorbed complexes: Ca^{2+} cations stabilize Eu(III)/(OH)/Ca complexes in the solution and on the surface: $CaEu(OH)_4(H_2O)_4^+$, $CaEu(OH)_4(H_2O)_{1.3}(>SiO)$, and $CaEu(OH)_3(H_2O)_2(>SiO)_2$. It can be seen they also stabilize Eu(III) as formally anionic $Eu(OH)_4$ species in cementitious environment. This is in line with the reported stability of the aqueous complexes $Ca_2[M(OH)_4]^{3+}$, and $Ca_3[M(OH)_6]^{3+}$ (with M = Nd, Cm) in hyperalkaline $CaCl_2$ solutions with Ca concentrations above

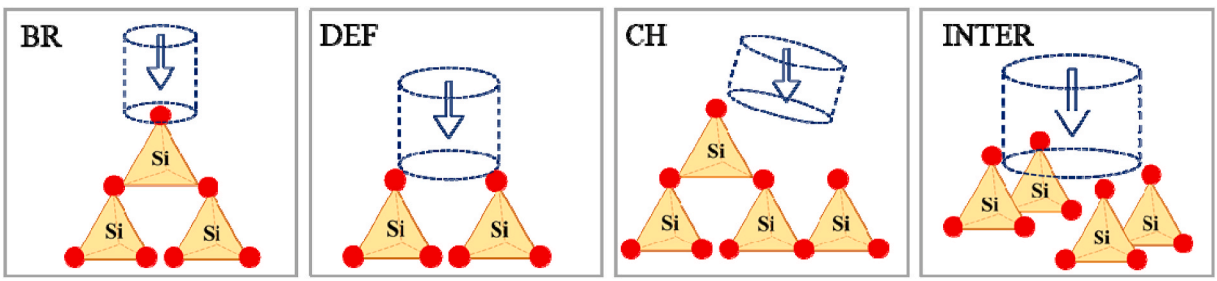

Fig. 1. Schematic representation of sorption sites on the (001) surface of C–S–H with high Ca/Si ratio: BR – bridging, DEF – defect, CH – chain, INTER – interchain.

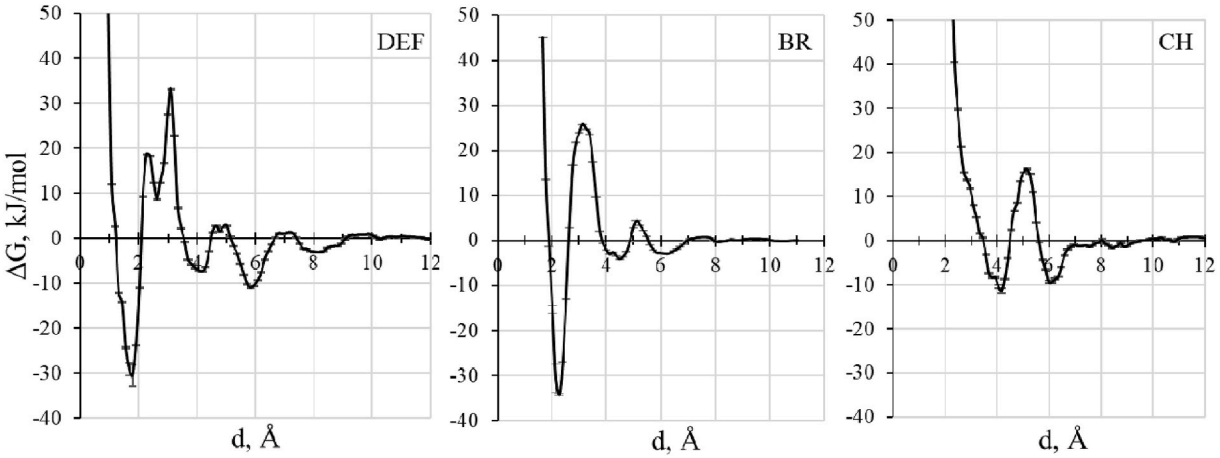

Fig. 2. PMF curves for Eu(III) sorption on the selected sorption sites of the (001) C–S–H surface (INTER site has been also evaluated, not shown here).

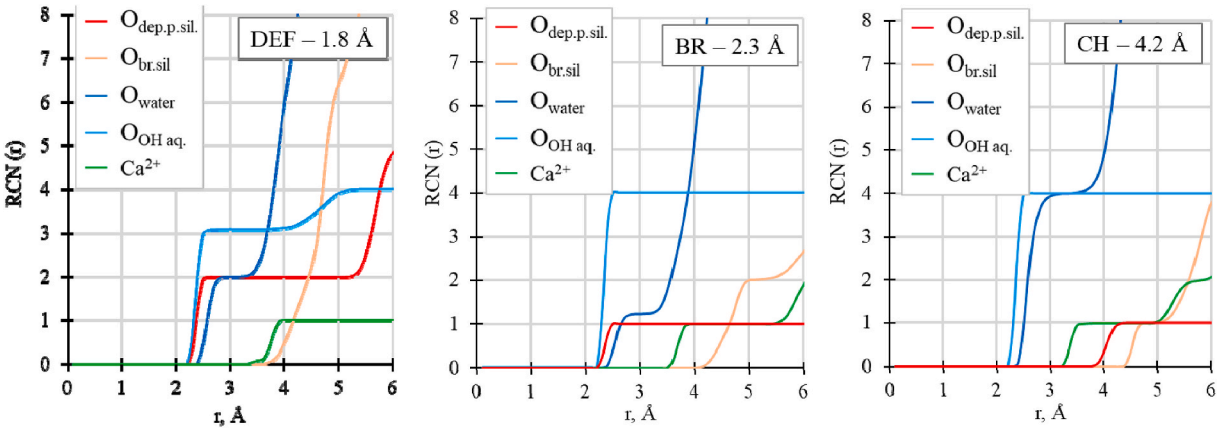

Fig. 3. Running coordination numbers for pairs of Eu(III) and different oxygens in the model system, and the Eu(III)/Ca^{2+} pair, calculated for the trajectories from PMF simulations at distances of the lowest energy minima for each site: DEF at 1.8 Å; BR at 2.3 Å, and CH at 4.2 Å from the surface (see Fig. 2).

0.05 M (Neck et al., 2009; Rojo et al., 2021).

3.2. Eu(III)-GLU sorption on C–S–H

Eu(III) forms stable complexes with gluconate, but the exact stoichiometry and stability of the complex remain ill-defined. Gluconate, with its multiple functional groups, offers various binding possibilities for cations. In this study, two plausible scenarios are examined. The first scenario involves the formation and sorption of the 1:1 complex at low gluconate concentrations. The exact binding sites on gluconate are unknown, so we propose coordination with the deprotonated carboxylic group and deprotonated α-hydroxyl group as the most probable, although the coordination with a second alcohol group can be also speculated (Giroux et al., 2000; Al-Sogair et al., 2011; Rojo et al., 2021; Zenker et al., 2025). The second scenario explores the formation and sorption of the 1:2 Eu(III)/GLU complex at high gluconate and Ca^{2+} concentrations. Strong evidence was already provided for the formation of ternary/quaternary Ca-Ln(III)/An(III)–OH-GLU complexes, and a complex geometry recently suggested for Nd(III) is adopted for this study (Rojo et al., 2021) with the stoichiometry defined as $Ca_3Eu(OH)(GLU_{-3H})_2(aq)$. Also, the formation of 1:2 Tc(IV)/GLU complexes ($[Tc(IV)(Glu_{-2H})_2(H_2O)_2]^{2-}$) was recently reported as the most likely Tc (IV)-gluconate species in aqueoues solutions (Polly et al., 2025). Additionally, for the later degradation stage of cement (the alteration stage III), characterized by C–S–H phases with a Ca/Si ratio of 0.8, it has been observed that the presence of gluconate has a negligible effect on Eu(III) uptake (Dettmann et al., 2023). This suggests the potential significance of Ca^{2+} in the uptake and complexation mechanisms, which we aim to investigate.

The results of the potential of mean force calculations for the Eu(III)/GLU 1:1 complex sorption on the defect (DEF), bridging (BR), and chain (CH) sorption sites are shown in Fig. 4 (green line), along with the results for Eu(III) sorption without gluconate (black line) for comparison. An energy minimum near the surface was identified solely for the bridging site at $d_{CSH\text{-}Eu} = 2.3$ Å, with $\Delta G \approx -25$ kJ/mol. In comparison to the reference system, this minimum is slightly shifted to the right by 0.2 Å away from the surface, it is shallower by 10 kJ/mol, and the energy barrier is lower by 20 kJ/mol. For the defect site, the complex was sorbed only as an outer-sphere complex, with minima observed at distances approximately 4 Å away from the sites. In the case of the chain site, the minimum at 4.3 Å was determined to be the inner-sphere complexation at the neighboring bridging site. Consequently, it can be concluded that, on average, there is no favorable sorption of Eu(III)/GLU 1:1 complex at the chain site.

The running coordination numbers for Eu(III) have been further calculated from trajectories at distances corresponding to the lowest minima in the PMF curves for three sorption sites. The results are illustrated in Fig. 5. The total coordination number of Eu(III) (CN around 7) is reduced due to the hindrances caused by coordination with four negatively charged aqueous hydroxyl groups and two functional groups of gluconate. Only one water molecule could be identified in the coordination sphere of Eu(III)-GLU complex, as seen in the outer-sphere complex coordination (Fig. 5, DEF-2.4 Å). A decrease in Eu(III) coordination number has been previously observed for complexes with

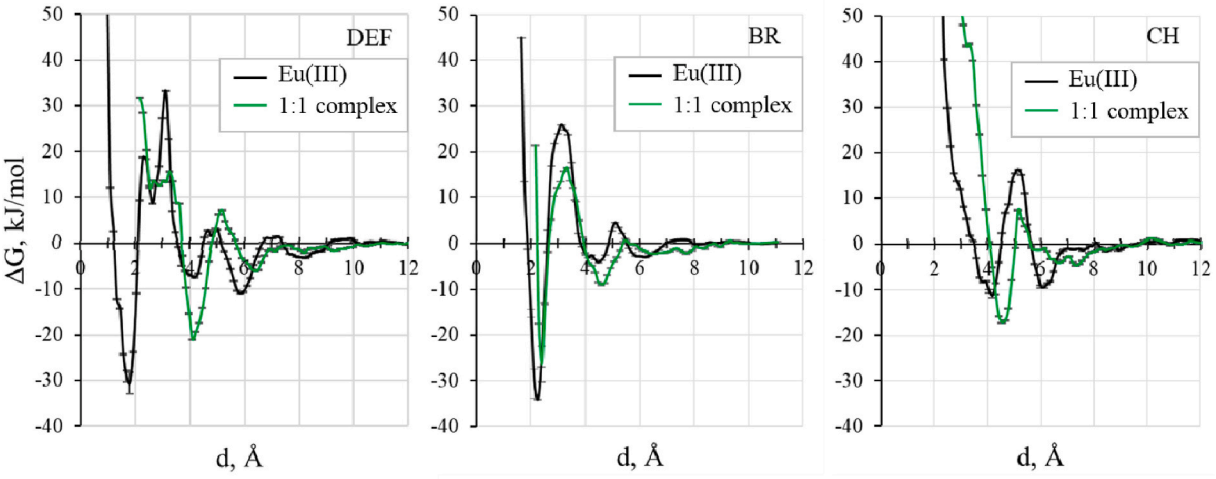

Fig. 4. PMF curves for sorption of Eu(III) and the 1:1 Eu(III)/GLU complex on three sorption sites of the (001) C–S–H surface.

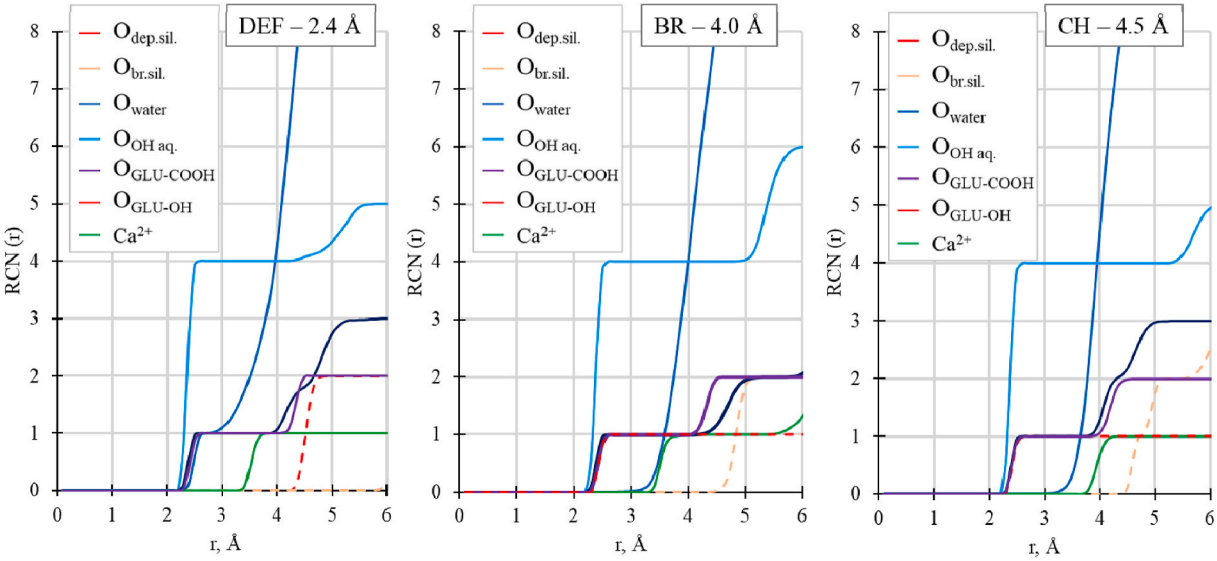

Fig. 5. Running coordination numbers for pairs of Eu(III) and different oxygens in the model system, and the Eu(III)/Ca^{2+} pair, calculated for the selected trajectories from PMF simulations at distances of the lowest energy minima for each site: DEF at 2.4 Å; BR at 4.0 Å, and CH at 4.5 Å from the surface (see Fig. 4).

multifunctional organic ligands (Atanassova et al., 2015; Dumpala et al., 2019). The inner-sphere surface complex of Eu(III)/GLU on the bridging site (Fig. 5, BR-4.0 Å) forms through exchange of water molecule for deprotonated silanol group ($RCN_{Eu\text{-}Odep.sil} = 1$ at $r \approx 2.4$ Å), while the number of aqueous hydroxyls remains the same ($RCN_{Eu\text{-}OHaq} = 4$ at $r \approx 2.3$ Å). It can be seen that the RCN for Eu(III) on the chain site (Fig. 5, CH-4.5 Å) are very close to those of the bridging site, because Eu(III) was strongly attracted to the neighboring deprotonated oxygen of bridging silicon ($RCN_{Eu\text{-}Odep.sil.} = 1$ at r ≈ 2.4 Å). In all analyzed trajectories, Ca^{2+} cations are found at distances of approximately 3.5 Å in the Eu(III) coordination sphere. They also participate in complex formation and further stabilize the $CaEu(OH)_4(H_2O)(GLU_{-H})$(>SiO) complex at the surface of C–S–H.

Taken together, these findings imply that the aqueous complex with gluconate is expected to sorb at low ligand concentrations, and sorption on the bridging site being the primary mechanism of adsorption for the 1:1 Eu(III)/GLU complex on the C–S–H surface as $CaEu(OH)_4(GLU_{-1H})$ (>Si–O). While the outer-sphere complexes formed on the defect sites may not be as strong as inner-sphere complexes, given the large number of defect sites on the surface, they would significantly contribute to Eu (III)-GLU uptake by C–S–H with high Ca/Si ratio. Similar observations were reported by Tasi et al. (2021) for Pu sorption on Portland cement in the presence of α-D-isosaccharinate (ISA). In their work, an increase of Pu uptake was observed for log ($[ISA]_{tot}$/M) ≈ - 3.5, and it was attributed to the co-adsorption of Pu (IV) with ISA on the cement surface. The formation of Ca(II)–Pu(IV)–OH–ISA surface complexes was then suggested.

The sorption of the 1:2 Eu(III)/GLU complex, $Ca_3Eu(OH)(GLU_{-3H})_2(aq)$, was analyzed for the two most favorable sorption sites: the defect site and the bridging site. The results of the new PMF calculations (brown line) are presented in Fig. 6 and compared to the previously discussed cases (green and black lines). It is evident that there is no significant minimum on the free energy of adsorption curve for both studied sites. The 1:2 Eu(III)/GLU complex does not approach the surface and is repulsed at $d_{CSH\text{-}Eu} = 6$ Å for the defect site and at $d_{CSH\text{-}Eu} =$ 4.5 Å for the bridging site.a.

It can be concluded that, once the Eu(III)/GLU complex forms in the solution, the mobility of Eu(III) on the surface of C–S–H increases, and the strength of sorption decreases. To better understand the behavior of Eu(III) in this multi-component system, the complexation of gluconate with already sorbed Eu(III) should also be evaluated. For this purpose, the distance between gluconate in the solution and sorbed Eu(III) was

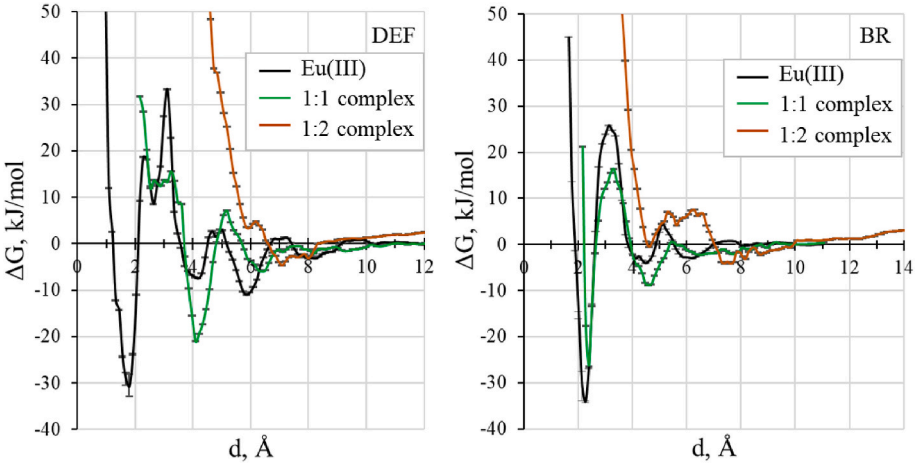

Fig. 6. PMF curves for sorption of the 1:1 and 1:2 Eu(III)/GLU complexes, and Eu(III) without gluconate on two sorption sites of the (001) C–S–H surface.

constrained. However, calculating one-dimensional PMF curves, as was done for direct sorption on the surface sites, was not possible because Eu (III) was detaching from the surface at distances less than 6 Å. Fixing Eu (III) at the sorption site would yield inaccurate results. Nevertheless, it provides an indirect evidence that gluconate is attracted to the surface of C–S–H and would interact with already sorbed Eu(III) increasing its mobility.

Taken together, these findings suggest that formation of the stable 1:2 Eu(III)/GLU complex in the solution and on the surface of C–S–H will hinder Eu(III) uptake by the cementitious materials. These results align well with experimental observations for the same system (Guidone, 2023): the presence of gluconate with concentrations higher than 0.01 M significantly decreases the sorption of Eu(III) on C–S–H phases with high Ca/Si ratio.

4. Conclusions

Molecular dynamic simulations and the potential of mean force calculations were used to study interaction mechanisms between Eu(III) and the (001) surface of C–S–H with a high Ca/Si ratio (1.4) in the absence and presence of gluconate. The most typical sorption sites for cations on the surface – bridging, defect, and chain sites – were considered and systematically investigated. The studies reveal that Eu (III) forms robust inner-sphere complexes with deprotonated silanol groups on the (001) surface of C–S–H. The presence of Ca(II) cations contributes to complex formation, enhancing the coordination of Eu(III) with multiple aqueous hydroxyl groups and functional groups of gluconate. These results are in good agreement with spectroscopic evidences available in the literature. Furthermore, gluconate demonstrates its capacity to create stable complexes with both Eu(III) and Ca(II) in both solution and on the C–S–H surface. Two main effects of gluconate presence on the sorption of Eu(III) on C–S–H phase with high Ca/Si ratio were identified. First, at low gluconate concentration, the sorption of the 1:1 Eu(III)-GLU complex takes place. This supports the notion that the ternary complex C–S–H/Eu(III)/GLU needs to be considered for the overall interpretation and understanding of the system. Second, at high ligand concentration, gluconate stabilizes Eu(III) in the aqueous phase as a ternary Ca–Eu(III)-GLU complex, preventing it from sorption on the surface. The findings of molecular dynamics simulations are consistent with reported experimental observations (Guidone, 2023; Guidone et al., 2024) and provide valuable insights into the complex interactions between Eu(III), Ca(II), gluconate, and the C–S–H surface, contributing to a better understanding of the sorption processes involved. The proposed approach can be extended to study the effect of organics on the sorption behavior of other metal ions of relevance in the context of the nuclear waste disposal, e.g., Am(III), on C–S–H phases with various Ca/Si ratios, characteristic for other degradation phases of cement.

CRediT authorship contribution statement

Iuliia Androniuk: Writing – review & editing, Writing – original draft, Visualization, Methodology, Investigation, Conceptualization. **Rosa Ester Guidone:** Writing – review & editing, Validation, Conceptualization. **Marcus Altmaier:** Writing – review & editing, Supervision, Project administration. **Xavier Gaona:** Writing – review & editing, Supervision, Project administration, Conceptualization.

Declaration of competing interest

The authors declare that they have no known competing financial interests or personal relationships that could have appeared to influence the work reported in this paper.

Acknowledgements

This work was supported by the German collaborative GRAZ II project (Geochemische Radionuklidrückhaltung an Zementalterationsphasen, Teilprojekt 02E11860C), funded by the German Federal Ministry for the Environment, Nature Conservation, Nuclear Safety and Consumer Protection (BMUV).

The authors likewise acknowledge support by the state of Baden-Württemberg through bwHPC and the German Research Foundation (DFG) through grant no INST 40/575-1 FUGG (JUSTUS 2 cluster).

Data availability

Data will be made available on request.

References

Al-Sogair, F.M., Operschall, B.P., Sigel, A., Sigel, H., Schnabl, J., Sigel, R.K.O., 2011. Probing the metal-ion-binding strength of the hydroxyl group. Chem. Rev. 111 (8), 4964–5003. https://doi.org/10.1021/cr100415s.

Androniuk, I., Kalinichev, A.G., 2020. Molecular dynamics simulation of the interaction of uranium (VI) with the C–S–H phase of cement in the presence of gluconate. Appl. Geochem. 113, 104496. https://doi.org/10.1016/j.apgeochem.2019.104496.

Atanassova, M., Kurteva, V., Billard, I., 2015. Coordination chemistry of Europium(III) ion towards acylpyrazolone ligands. Anal. Sci. 31 (9), 917–922. https://doi.org/10.2116/analsci.31.917.

Beaudoin, J.J., Raki, L., Alizadeh, R., 2009. A ^{29}Si MAS NMR study of modified C–S–H nanostructures. Cement Concr. Compos. 31, 585–590. https://doi.org/10.1016/j.cemconcomp.2008.11.004.

Berendsen, H.J.C., Grigera, J.R., Straatsma, T.P., 1987. The missing term in effective pair potentials. J. Phys. Chem. A 91, 6269–6271. https://doi.org/10.1021/j100308a038.

Bonaccorsi, E., Merlino, S., Kampf, A.R., 2005. The crystal structure of tobermorite 14 Å (Plombierite), a C−S−H phase. J. Am. Ceram. Soc. 88, 505–512. https://doi.org/10.1111/j.1551-2916.2005.00116.x.

Braun, E., Gilmer, J., Mayes, H.B., Mobley, D.L., Monroe, J.I., Prasad, S., Zuckerman, D. M., 2019. Best practices for foundations in molecular simulations [article v1.1]. Living J. Comput. Mol. Sci. 1 (5957). https://doi.org/10.33011/livecoms.1.1.5957.

Chiorescu, I., Kremleva, A., Krüger, S., 2022. On the sorption mode of U(IV) at calcium Silicate hydrate: Acomparison of adsorption, absorption in the interlayer, and incorporation by means of density functional calculations. Minerals 12, 1541. https://doi.org/10.3390/min12121541.

Churakov, S.V., Labbez, C., Pegado, L., Sulpizi, M., 2014. Intrinsic acidity of surface sites in calcium silicate hydrates and its implication to their electrokinetic. properties. J. Phys. Chem. C 118, 11752–11762. https://doi.org/10.1021/jp502514a.

Cong, X.D., Kirkpatrick, R.J., 1996. Si-29 MAS NMR Study of the structure of calcium silicate hydrate. Adv. Cement Base Mater. 3, 144–156. https://doi.org/10.1016/S1065-7355(96)90046-2.

Cygan, R.T., Liang, J.-J., Kalinichev, A.G., 2004. Molecular models of hydroxide, oxyhydroxide, and clay phases and the development of a general force field. J. Phys. Chem. B 108, 1255–1266. https://doi.org/10.1021/jp0363287.

Cygan, R.T., Greathouse, J.A., Kalinichev, A.G., 2021. Advances in clayff molecular simulation of layered and nanoporous materials and their aqueous interfaces. J. Phys. Chem. C 125, 17573–17589. https://doi.org/10.1021/acs.jpcc.1c04600.

Dario, M., Molera, M., Allard, B., 2006. Sorption of europium on TiO_2 and cement at high pH in the presence of organic ligands. J. Radioanal. Nucl. Chem. 270 (3), 495–505. https://doi.org/10.1007/s10967-006-0455-4.

Dumpala, R.M.R., Boda, A., Kumar, P., Rawat, N., Ali, Sk M., 2019. Reduction in coordination number of Eu(III) on complexation with pyrazine Mono- and Di-Carboxylates in aqueous medium. Inorg. Chem. 58 (16), 11180–11194. https://doi.org/10.1021/acs.inorgchem.9b01772.

Duque-Redondo, E., Yamada, K., Dolado, J.S., Manzano, H., 2021. Microscopic mechanism of radionuclide Cs retention in Al containing C-S-H nanopores. Comput. Mater. Sci. 190, 110312. https://doi.org/10.1016/j.commatsci.2021.110312.

Duque-Redondo, E., Bonnaud, P.A., Manzano, H., 2022. A comprehensive review of C-S-H empirical and computational models, their applications, and practical aspects. Cement Concr. Res. 156, 106784. https://doi.org/10.1016/j.cemconres.2022.106784.

Evans, N.D.M., 2008. Binding mechanisms of radionuclides to cement. Cement Concr. Res. 38, 543–553. https://doi.org/10.1016/j.cemconres.2007.11.004.

Fiorin, G., Klein, M.L., Henin, J., 2013. Using collective variables to drive molecular dynamics simulations. Mol. Phys. 111, 3345–3362.

Fralova, L., Lefevre, G., Made, B., Marsac, R., Thory, E., Dagnelie, R.V.H., 2021. Effect of organic compounds on the retention of radionuclides in clay rocks: mechanisms and specificities of Eu(III), Th(IV), and U(VI). Appl. Geochem. 127, 104859. https://doi.org/10.1016/j.apgeochem.2020.104859.

Frisch, M.J., Trucks, G.W., Schlegel, H.B., Scuseria, G.E., Robb, M.A., Cheeseman, J.R., Scalmani, G., Barone, V., Petersson, G.A., Nakatsuji, H., Li, X., Caricato, M., Marenich, A., Bloino, J., Janesko, B.G., Gomperts, R., Mennucci, B., Hratchian, H.P., Ortiz, J.V., Izmaylov, A.F., Sonnenberg, J.L., Williams-Young, D., Ding, F., Lipparini, F., Egidi, F., Goings, J., Peng, B., Petrone, A., Henderson, T., Ranasinghe, D., Zakrzewski, V.G., Gao, J., Rega, N., Zheng, G., Liang, W., Hada, M., Ehara, M., Toyota, K., Fukuda, R., Hasegawa, J., Ishida, M., Nakajima, T., Honda, Y., Kitao, O., Nakai, H., Vreven, T., Throssell, K., Montgomery Jr., J.A., Peralta, J.E., Ogliaro, F., Bearpark, M., Heyd, J.J., Brothers, E., Kudin, K.N., Staroverov, V.N., Keith, T., Kobayashi, R., Normand, J., Raghavachari, K., Rendell, A., Burant, J.C., Iyengar, S.S., Tomasi, J., Cossi, M., Millam, J.M., Klene, M., Adamo, C., Cammi, R., Ochterski, J.W., Martin, R.L., Morokuma, K., Farkas, O., Foresman, J.B., Fox, D.J., 2016. Gaussian 09, Revision C.01. Gaussian, Inc., Wallingford CT.

Giffaut, E., Grivé, M., Blanc, P., Vieillard, P., Colàs, E., Gailhanou, H., Gaboreau, S., Marty, N., Madé, B., Duro, L., 2014. Andra thermodynamic database for performance assessment: thermochimie. Appl. Geochem. 49, 225–236. https://doi.org/10.1016/j.apgeochem.2014.05.007.

Giroux, S., Rubini, P., Henry, B., Aury, S., 2000. Complexes of praseodymium(III) with D-gluconic acid. Polyhedron 19 (13), 1567–1574. https://doi.org/10.1016/S0277-5387(00)00422-8.

Glasser, F.P., Macphee, D., Atkins, M., Pointer, C., Cowie, J., Wilding, C.R., Mattingley, N.J., Evans, P.A., 1989. Immobilisation of Radwaste in Cement Based Matrices. Department of the Environment. No. DOE-RW–89.058.

Grangeon, S., Claret, F., Roosz, C., Sato, T., Gaboreau, S., Linard, Y., 2016. Structure of nanocrystalline calcium silicate hydrates: insights from X-ray diffraction, synchrotron X-ray absorption and nuclear magnetic resonance. J. Appl. Crystallogr. 49, 771–783. https://doi.org/10.1107/S1600576716003885.

Grangeon, S., Fernandez-Martinez, A., Baronnet, A., Marty, N., Poulain, A., Elkaïm, E., Roosz, C., Gaboreau, S., Henocq, P., Claret, F., 2017. Quantitative X-ray pair distribution function analysis of nanocrystalline calcium silicate hydrates: a contribution to the understanding of cement chemistry. J. Appl. Crystallogr. 50, 14–21. https://doi.org/10.1107/S1600576716017404.

Grossfield, A., 2014. An implementation of WHAM: the weighted histogram analysis method, Version 2.0.9. http://membrane.urmc.rochester.edu/wordpress/?page_id=126.

Grossfield, A., Patrone, P.N., Roe, D.R., Schulz, A.J., Siderius, D.W., Zuckerman, D.M., 2018. Best practices for quantification of uncertainty and sampling quality in molecular simulations [article V1.0]. Living. J. Comput. Mol. Sci. 1 (5067). https://doi.org/10.33011/livecoms.1.1.5067.

Guidone, R.E., 2023. Impact of Formate, Citrate and Gluconate on the Retention Behavior of Pu(III/IV), Cm(Iii) and Eu(Iii) by Cement Phases. Karlsruhe Institute of Technology. Doctoral Thesis.

Guidone, R.E., Gaona, X., Altmaier, M., Lothenbach, B., 2024. Gluconate and formate uptake by hydrated cement phases. Appl. Geochem. 175, 106145. https://doi.org/10.1016/j.apgeochem.2024.106145.

Humphrey, W., Dalke, A., Schulten, K., 1996. VMD: visual molecular dynamics. J. Mol. Graph. 14, 33–38. https://doi.org/10.1016/0263-7855(96)00018-5.

Jorgensen, W.L., Maxwell, D.S., Tirado-Rives, J., 1996. Development and testing of the OPLS all-atom force field on conformational energetics and properties of organic liquids. J. Am. Chem. Soc. 118 (45), 11225–11236. https://doi.org/10.1021/ja9621760.

Kalinichev, A.G., Wang, J.W., Kirkpatrick, R.J., 2007. Molecular dynamics modeling of the structure, dynamics and energetics of mineral-water interfaces: application to cement materials. Cement Concr. Res. 37, 337–347. https://doi.org/10.1016/j.cemconres.2006.07.004.

Kastner, J., 2011. Umbrella sampling. Wiley Interdiscip. Rev. Comput. Mol. Sci. 1, 932–942. https://doi.org/10.1002/wcms.66.

Keith-Roach, M.J., 2008. The speciation, stability, solubility and biodegradation of organic co-contaminant radionuclide complexes: a review. Sci. Total Environ. 396 (1), 1–11. https://doi.org/10.1016/j.scitotenv.2008.02.030.

Keith Roach, M., Shahkarami, P., 2021. *Organic Materials with the Potential for Complexation in SFR, the Final Repository for short-lived Radioactive Waste. Stockholm, Sweden: SKB*. Report R-21-03.

Kirkpatrick, R.J., Yarger, J.L., McMillan, P.F., Yu, P., Cong, X., 1997. Raman spectroscopy of C-S-H, tobermorite, and jennite. Adv. Cement Base Mater. 5 (3–4), 93–99. https://doi.org/10.1016/S1065-7355(97)00001-1, 199.

Kirkpatrick, R.J., Kalinichev, A.G., Hou, X., Struble, L., 2005a. Experimental and molecular dynamics modeling studies of interlayer swelling: water incorporation in kanemite and ASR gel. Mater. Struct. 38, 449–458. https://doi.org/10.1007/BF02482141.

Kirkpatrick, R.J., Kalinichev, A.G., Wang, J., 2005b. Molecular dynamics modelling of hydrated mineral interlayers and surfaces: structure and dynamics. Mineral. Mag. 69, 289–308. https://doi.org/10.1180/0026461056930251.

Kumar, A., Walder, B.J., Kunhi Mohamed, A., Hofstetter, A., Srinivasan, B., Rossini, A.J., Scrivener, K., Emsley, L., Bowen, P., 2017. The atomic-level structure of cementitious calcium silicate hydrate. J. Phys. Chem. C 121, 17188–17196. https://doi.org/10.1021/acs.jpcc.7b02439.

Kunhi Mohamed, A., Parker, S.C., Bowen, P., Galmarini, S., 2018. An atomistic building block description of C-S-H - towards a realistic C-S-H model. Cement Concr. Res. 107, 221–235. https://doi.org/10.1016/j.cemconres.2018.01.007.

Marmodee, B., Jahn, K., Ariese, F., Gooijer, C., Kumke, M.U., 2010. Direct spectroscopic evidence of 8- and 9-fold coordinated Europium(III) species in H_2O and D_2O. J. Phys. Chem. A 114 (50), 13050–13054. https://doi.org/10.1021/jp1094036.

Masara, F., Honorio, T., Benboudjema, F., 2023. Sorption in C-S-H at the molecular level: disjoining pressures, effective interactions, hysteresis, and cavitation. Cement Concr. Res. 164, 107047. https://doi.org/10.1016/j.cemconres.2022.107047.

Neck, V., Altmaier, M., Rabung, T., Lützenkirchen, J., Fanghänel, T., 2009. Thermodynamics of trivalent actinides and neodymium in NaCl, $MgCl_2$, and $CaCl_2$ solutions: solubility, hydrolysis, and ternary Ca–M(III)–OH complexes. Pure Appl. Chem. 81, 1555–1568. https://doi.org/10.1351/PAC-CON-08-09-05.

Ochs, M., Mailants, D., Wang, L., 2016. Radionuclide and Metal Sorption on Cement and Concrete, vol. 29. Springer. https://doi.org/10.1007/978-3-319-23651-3. ISBN: 978-3-319-23650-6.

Plimpton, S., 1995. Fast parallel algorithms for short-range molecular dynamics. J. Comput. Phys. 117, 1–19. https://doi.org/10.1006/jcph.1995.1039.

Pointeau, I., Piriou, B., Fedoroff, M., Barthes, M.-G., Marmier, N., Fromage, F., 2001. Sorption mechanisms of Eu^{3+} on CSH phases of hydrated cements. J. Colloid Interface Sci. 236, 252–259. https://doi.org/10.1006/jcis.2000.7411.

Polly, R., Dardenne, K., Duckworth, S., Gaona, X., Pruessmann, T., Rothe, J., Altmaier, M., Geckeis, H., 2025. *Ab Initio* speciation of Tc-Gluconate complexes in aqueous systems. Inorg. Chem. 64 (11), 5412–5423. https://doi.org/10.1021/acs.inorgchem.4c05115.

Rojo, H., Gaona, X., Rabung, T., Polly, R., García-Gutierrez, M., Missana, T., Altmaier, M., 2021. Complexation of Nd(III)/Cm(III) with gluconate in alkaline NaCl and $CaCl_2$ solutions: solubility, TRLFS and DFT studies. Appl. Geochem. 126, 104864. https://doi.org/10.1016/j.apgeochem.2020.104864.

Roosz, C., Vieillard, P., Blanc, P., Gaboreau, S., Gailhanou, H., Braithwaite, D., Montouillout, V., Denoyel, R., Henocq, P., Made, B., 2018. Thermodynamic properties of C-S-H, C-A-S-H and M-S-H phases: results from direct measurements and predictive modelling. Appl. Geochem. 92, 140–156. https://doi.org/10.1016/j.apgeochem.2018.03.004.

Schlegel, M.L., Pointeau, I., Coreau, N., Reiller, P.E., 2004. Mechanism of europium retention by calcium silicate hydrates: an EXAFS study. Environ. Sci. Technol. 38, 4423–4431. https://doi.org/10.1021/es0498989.

Szczerba, M., Kalinichev, A.G., 2016. Intercalation of ethylene glycol in smectites: several molecular simulation models verified by X-Ray diffraction data. Clays Clay Miner. 64 (4), 488–502. https://doi.org/10.1346/ccmn.2016.0640411.

Tasi, A., Gaona, X., Rabung, Th, Fellhauer, D., Rothe, J., Dardenne, K., Lützenkirchen, J., Grive, M., Colas, E., Bruno, J., Kallstrom, K., Altmaier, M., Geckeis, H., 2021. Plutonium retention in the isosaccharinate – cement system. Appl. Geochem. 126, 104862. https://doi.org/10.1016/j.apgeochem.2020.104862.

Tits, J., Stumpf, T., Rabung, T., Wieland, E., Fanghänel, T., 2003. Uptake of Cm(III) and Eu(III) by calcium silicate hydrates: a solution chemistry and time-resolved laser fluorescence spectroscopy study. Environ. Sci. Technol. 37, 3568–3573. https://doi.org/10.1021/es030020b.

Tu, Y., Yu, Q., Wen, R., Shi, P., Yuan, L., Ji, Y., Sas, G., Elfgren, L., 2021. Molecular dynamics simulation of coupled water and ion adsorption in the nano-pores of a

realistic calcium-silicate-hydrate gel. Constr. Build. Mater. 299, 123961. https://doi.org/10.1016/j.conbuildmat.2021.123961.

Veggel, F.C.J.M., Reinhoudt, D.N., 1999. New, accurate Lennard-Jones parameters for trivalent lanthanide ions, tested on [18]Crown-6. Chem. Eur J. 5 (1). https://doi.org/10.1002/(SICI)1521-3765(19990104)5:1<90::AID-CHEM90>3.0.CO;2-8.

Wieland, E., 2014. Sorption Data Base for the Cementitious near Field of L/ILW and ILW Repositories for Provisional Safety Analyses for SGT-E2. (Nagra: Technical Report, Report No.: 14-08). National Cooperative for the Disposal of Radioactive Waste (Nagra).

Zenker, S., Lohmann, J., Chiorescu, I., Krüger, S., Kumke, M.U., Reich, T., Schmeide, K., Kretzschmar, J., 2025. Complexation of Ln(III) ions by gluconate: joint investigation applying TRLFS, CE-ICP-MS, NMR, and DF calculations. Inorg. Chem. 64 (16), 7970–7987. https://doi.org/10.1021/acs.inorgchem.4c05476.

Zhao, H., Yang, Y., Shu, X., Qiao, M., Dong, L., Ran, Q., 2024. Computational simulations of adsorption behavior of anionic surfactants at the portlandite–water interface under sulfate and calcium ions. Langmuir 40 (7), 3911–3922. https://doi.org/10.1021/acs.langmuir.3c03914.